Mühendis ve Makina / Engineer and Machinery
https://dergipark.org.tr/tr/pub/muhendismakina

DEVELOPMENT AND VERİFİCATİON OF A MULTİBLOCK STRUCTURED GRİD SOLVER FOR 3D EULER/NAVİER-STOKES EQUATİONS

Defne KIRAN[1], Ali Ruhşen ÇETE[2]

[1]Türk Hava Kurumu Üniversitesi, Havacılık ve Uzay Mühendisliği Fakültesi, Uçak Mühendisliği Bölümü, Ankara, ORCID No : http://orcid.org/0000-0003-2654-9686

[2]Türk Hava Kurumu Üniversitesi, Havacılık ve Uzay Mühendisliği Fakültesi, Uçak Mühendisliği Bölümü, Ankara, ORCID No : http://orcid.org/0000-0002-5877-4223

Keywords

Euler solver, multiblock solver, LU-ADI

Abstract

A multiblock structured grid solver for 3D Euler/Navier-Stokes equations is developed in this study. The solver employs the finite difference method together with the lower-upper factored scheme to provide fast solutions, while the use of multiblock structured grids allows the algorithm to be applied to complex geometries.

The developed solver is then tested on a "body-only" axisymmetric model with a single-engine fighter aft-end which was previously investigated experimentally. The numerical results of the pressure distributions on the model's body obtained by the solver are compared to the experimental results. The numerical and experimental results were found to be in good agreement, indicating that the solver can sufficiently solve the flow equations, and represent the physical properties of the flow.

[1] Sorumlu yazar; e-posta: dkiran@thk.edu.tr
doi : muhendismakina.1319195

ÜÇ BOYUTLU EULER/NAVİER-STOKES DENKLEMLERİ İÇİN ÇOK BLOKLU YAPISAL AĞLI ÇÖZÜCÜ GELİŞTİRİLMESİ VE DOĞRULANMASI

Anahtar kelimeler

Euler çözücü, çok bloklu çözücü, yukarı-aşağı yaklaşık çarpanlarına ayırma

Öz

Bu çalışmada üç boyutlu Euler-Navier Stokes denklemleri için çok boyutlu yapısal ağlı bir çözücü geliştirilmiştir. Çözücü, denklem çözümleri için sonlu farklar metodu ve yukarı-aşağı yaklaşık çarpanlarına ayırma algoritması kullanmaktadır. Çok bloklu yapısal ağ kullanımı ise algoritmanın kompleks geometriler için kullanımına olanak sağlamaktadır. Geliştirilen çözücünün doğruluğu, daha önce deneysel olarak test edilen tek motor arka gövde etkileşimi sonuçlarıyla karşılaştırılmıştır. Geliştirilen çözücünün kullanımıyla elde edilen sayısal veriler, deneysel verilerle uyumluluk gösterdiğinden, geliştirilen çözücünün akış fiziğini yeteri kadar temsil edebildiği gösterilmiştir.

Araştırma Makalesi
Başvuru Tarihi : 17.02.2023
Kabul Tarihi : 17.03.2023

Research Article
Submission Date : 17.02.2023
Accepted Date : 17.03.2023

1. Introduction

The use of numerical methods in the solution of aerodynamic engineering problems provides great convenience when compared to experimental studies. It is not always feasible to reproduce an entire system to test in wind tunnels, and even so, experimental testing requires time and is a costly process. On the other hand, it is possible to quickly evaluate and apply the modifications proposed during the design process, using numerical methods. For this reason, numerical aerodynamic analyses gain great importance in the overall design process, from conceptual design to detailed design, and it is of great importance to develop a solver that can quickly and accurately model aerodynamic analyzes of complex geometric structures.

Solvers for three-dimensional (3D) Euler/Navier Stokes equations of compressible flows were developed in several different studies. The foundations on this subject were laid by the pioneering work of Pulliam and Steger (1980). They developed an implicit, finite difference method to solve compressible unsteady inviscid or thin-layered viscous 3D flows, which provided reasonably accurate solutions for simple aerodynamic configurations. Obayashi and Fujii (1985) successfully applied the lower-upper alternating-direction implicit (LU-ADI) factored scheme to solve the thin layer Navier-Stokes equations. Other studies applied these methods to multiblock structured grids (Leyland & Vos, 1995; Rizzi et al., 1993; Siclari et al., 1989; Yadlin & Caughey, 1991).

The use of multiblock structured grids in numerical analysis has many advantages. By decomposing the grids into a number of topologically simpler blocks, it is straightforward to conduct numerical analyses of complex geometries and flows (Blazek, 2005). Since each block can be solved independently of the others, the multi-block approach can easily be applied to parallel computing (Takaki et al., 2002). The computational time can be greatly reduced in this manner.

This study aims to develop a 3D multiblock Euler/Navier Stokes equations solver, using the finite difference method and lower-upper (LU) factored scheme, and to verify the accuracy of the solver by comparing it with the experimental data. A multiblock structured grid, consisting of two blocks, is used for the computational domain. The numerical results obtained by the solver are compared to Berrier's experimental work on AGARD AR-303 (Berrier, 1994). The pressure coefficients along the body of the model are considered for the comparison of the numerical and experimental data.

2. Formulation of the Numerical Method

The nondimensionalized form of the three-dimensional Navier-Stokes equations

for an unsteady compressible viscous flow in the curvilinear space (ξ,η,ζ,τ) can be written as

$$\partial_\tau \hat{q} + \partial_\xi \hat{E} + \partial_\eta \hat{F} + \partial_\zeta \hat{G} = k\partial_\zeta \hat{S}/Re \quad (1)$$

where

$$\hat{q} = J^{-1}\begin{bmatrix}\rho\\ \rho u\\ \rho v\\ \rho w\\ e\end{bmatrix}, \quad \hat{E} = J^{-1}\begin{bmatrix}\rho U\\ \rho uU + \xi_x p\\ \rho vU + \xi_y p\\ \rho wU + \xi_z p\\ (e+p)U - \xi_t p\end{bmatrix}, \quad \hat{F} = J^{-}\begin{bmatrix}\rho V\\ \rho uV + \eta_x p\\ \rho vV + \eta_y p\\ \rho wV + \eta_z p\\ (e+p)V - \eta_t p\end{bmatrix}, \quad \hat{G} = J^{-1}\begin{bmatrix}\rho W\\ \rho uW + \zeta_x p\\ \rho vW + \zeta_y p\\ \rho wW + \zeta_z p\\ (e+p)W - \zeta_t p\end{bmatrix},$$

$$\hat{S} = J^{-1}\begin{bmatrix}0\\ \mu\left(\zeta_x^2+\zeta_y^2+\zeta_z^2\right)u_\zeta + (\mu/3)\left(\zeta_x u_\zeta + \zeta_y v_\zeta + \zeta_z w_\zeta\right)\zeta_x\\ \mu\left(\zeta_x^2+\zeta_y^2+\zeta_z^2\right)v_\zeta + (\mu/3)\left(\zeta_x u_\zeta + \zeta_y v_\zeta + \zeta_z w_\zeta\right)\zeta_y\\ \mu\left(\zeta_x^2+\zeta_y^2+\zeta_z^2\right)w_\zeta + (\mu/3)\left(\zeta_x u_\zeta + \zeta_y v_\zeta + \zeta_z w_\zeta\right)\zeta_z\\ \left\{\left(\zeta_x^2+\zeta_y^2+\zeta_z^2\right)\left[0.5\mu(u^2+v^2+z^2)_\zeta + \kappa Pr^{-1}(\gamma-1)^{-1}(a^2)_\zeta\right]\right.\\ \left.+(\mu/3)\left(\zeta_x u + \zeta_y v + \zeta_z w\right)\times\left(\zeta_x u_\zeta + \zeta_y v_\zeta + \zeta_z w_\zeta\right)\right\}\end{bmatrix} \quad (2)$$

and k=0 for inviscid flow, and k=1 for viscous flow. μ is the dynamic viscosity, and Re and Pr represent the Reynolds and Prandtl numbers, respectively. U,V and W terms in Eqs. 1 are defined as

$$U=\xi_t+\xi_x u+\xi_y v+\xi_z w$$

$$V=\eta_t+\eta_x u+\eta_y v+\eta_z w \quad (3)$$

$$W=\zeta_t+\zeta_x u+\zeta_y v+\zeta_z w$$

and the pressure term, p is defined as follows:

$$p=(\gamma\text{-}1)[e\text{-}0.5(u^2+v^2+w^2)] \quad (4)$$

where γ is the specific heat ratio of the ideal gas, and is equal to 1.4. The speed of sound term, a in Eq. 2 is expressed by using the ideal gas law, as follows:

$$a = \sqrt{\gamma p/\rho} \quad (5)$$

The metrics required to solve Eqs. 1 are as follows:

$$\xi_x = J\left(y_\eta z_\zeta - y_\zeta z_\eta\right) \qquad \eta_x = J\left(z_\xi y_\zeta - y_\xi z_\zeta\right)$$

$$\xi_y = J\left(z_\eta x_\zeta - z_\zeta x_\eta\right) \qquad \eta_x = J\left(x_\xi z_\zeta - x_\zeta z_\xi\right)$$

$$\xi_z = J\left(x_\eta y_\zeta - y_\eta x_\zeta\right) \qquad \eta_z = J\left(y_\xi x_\zeta - x_\xi y_\zeta\right)$$

$$\zeta_x = J\left(y_\xi z_\eta - z_\xi y_\eta\right) \qquad \xi_t = -x_\tau \xi_x - y_\tau \xi_y - z_\tau \xi_z$$

$$\zeta_y = J\left(x_\eta z_\xi - x_\xi z_\eta\right) \qquad \eta_t = -x_\tau \eta_x - y_\tau \eta_y - z_\tau \eta_z$$

$$\zeta_x = J\left(x_\xi y_\eta - y_\xi x_\eta\right) \qquad \xi_t = -x_\tau \zeta_x - y_\tau \zeta_y - z_\tau \zeta_z$$

$$J^{-1} = x_\xi y_\eta z_\zeta + x_\zeta y_\xi z_\eta + x_\eta y_\zeta z_\xi - x_\xi y_\zeta z_\eta - x_\eta y_\xi z_\zeta - x_\zeta y_\eta z_\xi$$

The interior points are evaluated using the second-order central difference method, and the boundaries are evaluated using three-point one-sided formulas. The nondimensionalization of the Eqs. 1 is realized by the following terms:

$$\bar{\rho} = \frac{\rho}{\rho_\infty}, \quad \bar{u} = \frac{u}{u_\infty}, \quad \bar{v} = \frac{v}{v_\infty}, \quad \bar{e} = \frac{e}{\rho_\infty a^2}, \quad \bar{p} = \frac{p}{\rho_\infty a^2}, \quad \bar{t} = \frac{ta}{l}, \quad \bar{\mu} = \frac{\mu}{\mu_\infty}, \quad Re = \frac{\rho_\infty l a_\infty}{\mu_\infty}$$

where the subscript ∞ corresponds to the freestream conditions and l corresponds to the reference length.

An implicit method is chosen to solve the Eqs. 1, since implicit methods can help to avoid the restrictive stability conditions of the time-step size when using small grid sizes. Applying this implicit method to Eqs. 1 yields:

$$\Delta\hat{Q}^n + h\left(\hat{E}_\xi^{n+1} + \hat{F}_\eta^{n+1} + \hat{G}_\zeta^{n+1} - Re^{-1}\hat{S}_\zeta^{n+1}\right) = 0 \tag{6}$$

where n corresponds to the time-step, and the first term on the left-hand side of the equation is expressed as follows:

$$\Delta\hat{Q}^n = \hat{Q}^{n+1} - \hat{Q}^n \tag{7}$$

and $\hat{Q}^n = \hat{Q}(n\Delta t)$.

The flux vectors, E,F,G, and S, which are the nonlinear functions of Q can be expressed using the Taylor expansion as follows:

$$\begin{aligned}
\hat{E}^{n+1} &= \hat{E}^n + \hat{A}^n\Delta\hat{Q}^n + O(h^2) \\
\hat{F}^{n+1} &= \hat{F}^n + \hat{B}^n\Delta\hat{Q}^n + O(h^2) \\
\hat{G}^{n+1} &= \hat{G}^n + \hat{C}^n\Delta\hat{Q}^n + O(h^2) \\
Re^{-1}\hat{S}^{n+1} &= Re^{-1}\left[\hat{S}^n + J^{-1}\hat{M}^n\Delta\hat{Q}^n\right] + O(h^2)
\end{aligned} \tag{8}$$

The delta-form is derived by substituting Eqs. 7 and 8 into Eq. 6, as follows:

$$\left[I + h\partial_\xi\hat{A}^n + h\partial_\eta\hat{B}^n + \partial_\zeta\hat{C}^n - Re^{-1}hJ^{-1}\hat{M}^n\right]\Delta\hat{Q}^n = -h\left(\hat{E}_\xi^n + \hat{F}_\eta^n + \hat{G}_\zeta^n - Re^{-1}\partial_\zeta\hat{S}^n\right) \tag{9}$$

Spatial partial derivatives are discretized using second-order central-difference

method. In this way, the algorithm becomes second-order accurate in space, and first-order accurate in time. The solver developed in this study uses the implicit factorization method (Beam and Warming, 1976, 1978; Briley and McDonald, 1973; Lindemuth and Killeen, 1973; Pulliam and Steger, 1980) and the LU-ADI scheme (Beam and Warming, 1976, 1978; Obayashi and Fujii, 1985) to solve the Eq. 9. The stability problem arising from the non-linear terms is solved by adding artificial dissipation terms to the algorithm.

3. Grid Structure and Boundary Conditions

The numerical method developed in this study is tested by using the "body-only" axisymmetric model with a single-engine fighter aft-end with convergent divergent nozzles, as described by Berrier (1994). The planform view of the tested model can be seen in Figure 1.

Figure 1 Planform View of Model Configurations Tested (adapted from Berrier (1994)). Dimensions are in Fractions Of Body Length (L)

A semi-cylinder is used to model the flow around the model. The length of the model is taken as 1.0L, and the semi-cylinder is 5.0L in length and 4.0L in diameter. Even though the geometry of the model is simple, the flow has complex characteristics, especially in the exhaust region. That is why, this region is meshed using different blocks. Figure 2 shows the multiblock structured grid used in this study. The multiblock structured grid consists of a block named as 2nd Block, and shown with green lines, and another block, named as 1st Block, shown with red lines in Figure 2. The 2nd block starts as in the form of an O-grid structure around a single axis at the inlet, at x = -1L, passing around the body, which is placed along the axis of the cylinder at x = 0, and continuing till the outlet (x = 4L). The 1st Block rotates around a single line, at the exhaust region, starting at the tail of the model and continuing till the outlet. The grids at points very close to the model's boundaries have fine mesh size, while the grid size increases towards the outer boundaries.

Next, the boundary conditions are defined for the multiblock structured grid. It is very important to define the boundary conditions correctly, and to provide relevant information at each block's boundaries. The boundary conditions for this

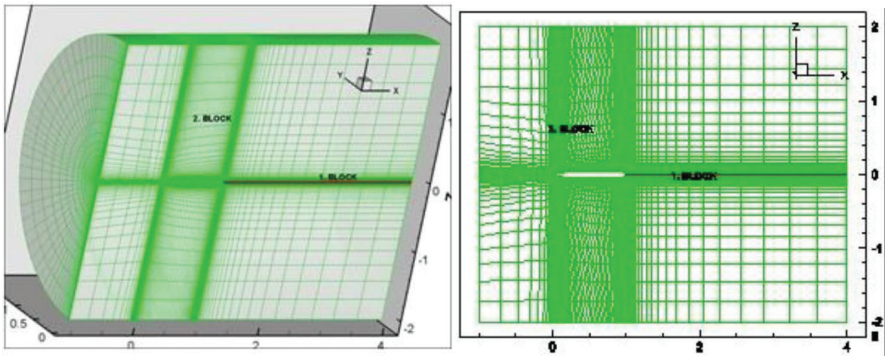

(a) (b)

Figure 2. Grid Structure Used for the Computational Domain in a 3D view (a) and an Orthographic View at the Plane, y = 0 (b)

study are based on the experimental study of Berrier (1994), since the results of this numerical simulation are compared to the experimental results of that study. In his experiments, Berrier (1994) uses jet-exhaust total pressures (p_e), which are nondimensionalized by the static pressure of the free stream ($p_{0,\infty}$). Values of velocity, density, and energy at the boundaries are set using these pressure ratios, assuming the flow is isentropic. For an isentropic flow, the Mach number (M) is calculated as follows:

$$M = \sqrt{\left\{\left(\frac{P_e}{P_{0,\infty}}\right)^{\frac{\gamma-1}{\gamma}} - 1\right\}\frac{2}{\gamma-1}} \tag{10}$$

Using Eq. 10, the velocity at the inlet boundary is set, and the density and pressure are set from the following equations:

$$\rho/\rho_\infty = \left(1+\frac{\gamma-1}{2}M_\infty^2\right)^{\frac{\gamma}{\gamma-1}} \Big/ \left(1+\frac{\gamma-1}{2}M^2\right)^{\frac{\gamma}{\gamma-1}} \tag{11}$$

$$\frac{P_e}{P_\infty} = \frac{P_e}{P_{0,\infty}}\left(1+\frac{\gamma-1}{2}M_\infty^2\right)^{\frac{\gamma}{\gamma-1}} \tag{12}$$

In this study, the Mach number at the inlet (x=- L) is taken as 0.9, outlet boundary is defined as a pressure outlet, and the pressure ratio of jet exhaust to outlet boundary is taken as 2.0. The plane at y = 0 is defined as symmetry boundary condition. Research and publication ethics were adhered to in this study.

4. Results and Discussion

Figure 3a shows the pressure distribution in terms of pressure coefficient, $c_{p,}$ over the body and the symmetry plane at y = 0. Figure 3b shows a close-up image of the pressure distribution, around the exhaust region, where the flow is expected to be complex.

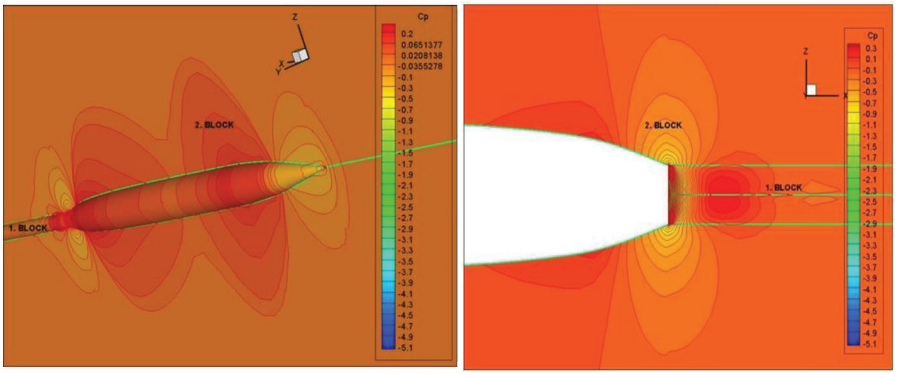

(a) (b)

Figure 3. Pressure Distribution in Terms of Pressure Coefficient c_p Over the Body and at the Symmetry Plane at y = 0 (a), and Around the Exhaust Region at y = 0 (b)

Figure 4 shows the comparison of the numerical data and experimental data of pressure coefficients on the body of axisymmetric single-engine fighter. Horizontal axis shows the axial distance downstream from the nose (x), nondimensiona-

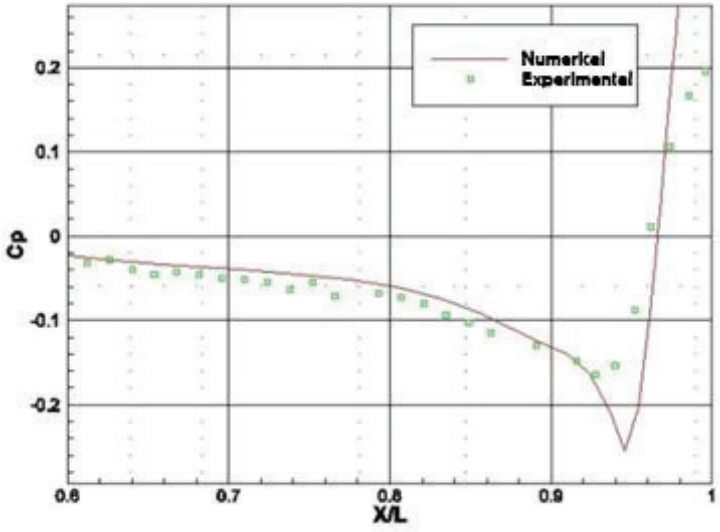

Figure 4. Numerical and Experimental Data of Pressure Coefficients (c_p) Along the Body of Axisymmetric Single-Engine Fighter

lized by the model length (L), and the vertical axis shows the pressure coefficients (c_p). The figure shows that the numerical results, obtained by the solver developed in this study, is in agreement with the experimental results. This shows that the 3D solver developed in this study can sufficiently represent the flow around the tested model.

5. Conclusion

In this study, a multiblock structured grid solver for 3D Euler/Navier-Stokes equations was developed. The solver uses the finite difference method together with LU scheme, which gives fast solutions, while the applicability of the multiblock structured grids allows the algorithm to be used for complex geometries.

The developed solver was then tested on a "body-only" axisymmetric model with a single-engine fighter aft-end with convergent divergent nozzles. This model was previously investigated experimentally by Berrier (1994). The numerical results of the pressure distributions on the body of the model, were compared to the experimental results. The numerical and the experimental results were found to be in agreement with each other, showing that the solver can sufficiently solve the equations of the flow, and can represent the flow physics.

References

Beam, R. M., Warming, R. F. (1976). An Implicit Finite-difference Algorithm for Hyperbolic Systems in Conservation-law Form. *Journal of Computational Physics,* 22(1), 87–110. https://doi.org/https://doi.org/10.1016/0021-9991(76)90110-8

Beam, R. M., Warming, R. F. (1978). An Implicit Factored Scheme for the Compressible Navier-Stokes Equations. *AIAA Journal,* 16(4), 393–402. https://doi.org/10.2514/3.60901

Berrier, B. L. (1994). Single-Engine Tail Interference Model. In *A Selection of Experimental Test Cases for the Validation of CFD Codes* (Vol. 2, Issue 303, pp. 452–475). NTRS-NASA.

Blazek, J. (2005). Introduction. *In Computational Fluid Dynamics: Principles and Applications* (pp. 1–4). Elsevier. https://doi.org/10.1016/B978-008044506-9/50003-5

Briley, W. R., Mcdonald, H. (1977). Solution of the Multidimensional Compressible Navier-Stokes Equations by a Generalized Implicit Method. *Journal of Computational Physics, 24,* 312–397.

Leyland, P., Vos, J. B. (1995). NSMB: A Modular Navier-Stokes Multiblock Code for CFD. *33rd Aerospace Sciences Meeting and Exhibition.* https://doi.org/https://doi.org/10.2514/6.1995-568

Lındemuth, I., Killeen, J. (1973). Alternating Direction Implicit Techniques for Two-dimensional Magnetohydrodynamic Calculations. *Journal of Computational Physics, 13(2)*, 181–208. https://doi.org/https://doi.org/10.1016/0021-9991(73)90022-3

Obayashi, S., Fujıı, K. (1985). Computation of Three-Dimensional Viscous Transonic Flows with the LU Factored Scheme. *7th Computational Physics Conference,* 192–202.

Pulliam, T. H., Steger, J. L. (1980). Implicit Finite-Difference Simulations of Three-Dimensional Compressible Flow. *AIAA Journal, 18(2),* 159–167. https://doi.org/10.2514/3.50745

Rizzi, A., Eliasson, P., Ingemar Lındblad, I., Charles Hırsch, I., Lacor, C., and Haeuser, J. (1993). The Engineering of Multiblock/Multigrid Software for Navier-Stokes Flows on Structured Meshes. *Computers Fluids, 22(3),* 341–367.

Sıcları, M., Delguıdıce, P., and Jameson, A. (1989). A Multigrid Finite Volume Method for Solving the Euler and Navier-Stokes Equations for High Speed Flows. *27th Aerospace Sciences Meeting.* https://doi.org/10.2514/6.1989-283

Takaki, R., Makida, M., Yamamoto, K., Yamane, T., Enomoto, S., Yamazakı, H., Iwamiya, T., and Nakamura, T. (2002). Current Status of CFD Platform - UPACS -. In P. Wilders, A. Ecer, N. Satofuka, J. Periaux, & P. Fox (Eds.), *Parallel Computational Fluid Dynamics 2001* (pp. 339–346). North-Holland. https://doi.org/https://doi.org/10.1016/B978-044450672-6/50094-3

Yadlin, Y., Caughey, D. A. (1991). Block Multigrid Implicit Solution of the Euler Equations of Compressible Fluid Flow. *AIAA Journal, 29(5)*, 712–719. https://doi.org/10.2514/3.10645